

# Preparation, Crystal Structure, and Vibrational Spectra of Perovskite-Type Mixed Oxides $\text{LaM}_y\text{M}'_{1-y}\text{O}_3$ ( $M, M' = \text{Mn, Fe, Co}$ )

Yue Wu,<sup>1</sup> Zuolong Yu, and Shetian Liu<sup>2</sup>

Changchun Institute of Applied Chemistry, Academia Sinica, Changchun 130022, People's Republic of China

Received April 19, 1993; in revised form November 10, 1993; accepted November 11, 1993

Three series of samples  $\text{LaMn}_y\text{Co}_{1-y}\text{O}_{3\pm\lambda}$ ,  $\text{LaFe}_y\text{Mn}_{1-y}\text{O}_{3\pm\lambda}$ , and  $\text{LaFe}_y\text{Co}_{1-y}\text{O}_{3\pm\lambda}$  ( $y = 0.0$  to  $1.0$ ) with Perovskite structure were prepared by an explosion method different from the generally used ceramic techniques. The variation of crystal structure, the infrared spectra, and the relationship between them were discussed in detail. The change of infrared absorption reflects the change of the crystal structure and the mixing of transition metals on B sites significantly influences the strength of the B-O bond. These influences are attributed to geometrical effects for  $\text{LaFe}_y\text{Mn}_{1-y}\text{O}_{3\pm\lambda}$  and  $\text{LaFe}_y\text{Co}_{1-y}\text{O}_{3\pm\lambda}$  and to electronic effects for  $\text{LaMn}_y\text{Co}_{1-y}\text{O}_{3\pm\lambda}$ . © 1994 Academic Press, Inc.

873 K for 1 hr and then by shaping and calcining in air at 1223 K for 6 hr.

**Crystal structure investigation.** The perovskite-type structure of the samples was verified by X-ray diffraction on a Shimadzu automatic recording X-ray diffractometer (type VD-1A) operating at 40 kV, with a working current of 10 mA, using  $\text{CuK}\alpha$  radiation in combination with a nickel filter.

**IR measurement.** IR spectra in the range 800–200  $\text{cm}^{-1}$  were recorded on a U.S.-made 580-B spectrophotometer. Samples were produced in the form of KBr pellets.

## INTRODUCTION

The mixed transition metal oxides with perovskite-type structure have been of great interest for many years as inorganic materials and catalysts (1). Among all perovskites functioning as complete oxidation catalysts, the compounds containing transition metal Mn, Fe, Co, or Ni in a B site are the best, as characterized by either the physicochemical properties or the catalytic properties (2). As for infrared spectra of these compounds, most of the work involved the titanates (3–5), zirconates (6), and some ordered perovskites (7, 8). Subba *et al.* (9) have reported the infrared and electronic spectra of chromites, manganites, and ferrites. Our present work deals mainly with the relation between crystal structure and infrared spectra of perovskite-type oxides with two transition metals on the B sites.

## EXPERIMENTAL

**Preparation.** Samples were prepared by evaporating the aqueous solution of mixed metal nitrates with citric acid to the explosion point, followed by decomposing at

<sup>1</sup> To whom correspondence should be addressed.

<sup>2</sup> Present address: Dalian Institute of Chemical Physics, Chinese Academy of Sciences, P.O. Box 110, Dalian 116023, People's Republic of China.

## RESULTS AND DISCUSSION

### Crystal Structure

The XRD patterns showed that all samples are single-phase perovskites, but, depending on the nature of transition metal element, these are distorted from their regular cubic to the hexagonal (H) (for  $\text{LaMnO}_3$  and Mn-rich samples), rhombohedral (R) (for  $\text{LaCoO}_3$  and Co-rich samples), or orthorhombic (O) (for  $\text{LaFeO}_3$  and Fe-rich samples) form. In each case, the transformation of the crystal phases generally occurs at  $y = 0.5$ . For the Mn-Co system, an orthorhombic transition phase occurs in the range  $0.5 \leq y \leq 0.7$ . Figure 1 illustrates the change of both the crystal phase and the lattice parameters with respect to the sample composition. A low degree of doping gives rise to different variations in lattice parameters while keeping the crystal phase unchanged. The increase of lattice parameters of Fe-doped  $\text{LaMnO}_3$  and  $\text{LaCoO}_3$  and the decrease of parameters of Co- and Mn-doped  $\text{LaFeO}_3$  seem to be correlated with their ionic radii:  $\text{Mn}^{3+}$  ( $r = 0.65 \text{ \AA}$ ) and  $\text{Fe}^{3+}$  ( $r = 0.64 \text{ \AA}$ ) ions have the same ionic radius but  $\text{Co}^{3+}$  ( $r = 0.61 \text{ \AA}$  for high spin state and  $0.56 \text{ \AA}$  for low spin state) is smaller (9); hence, variations of the lattice parameter for the Fe-Mn system (0.12%) were smaller than those for the Fe-Co system (0.25%).

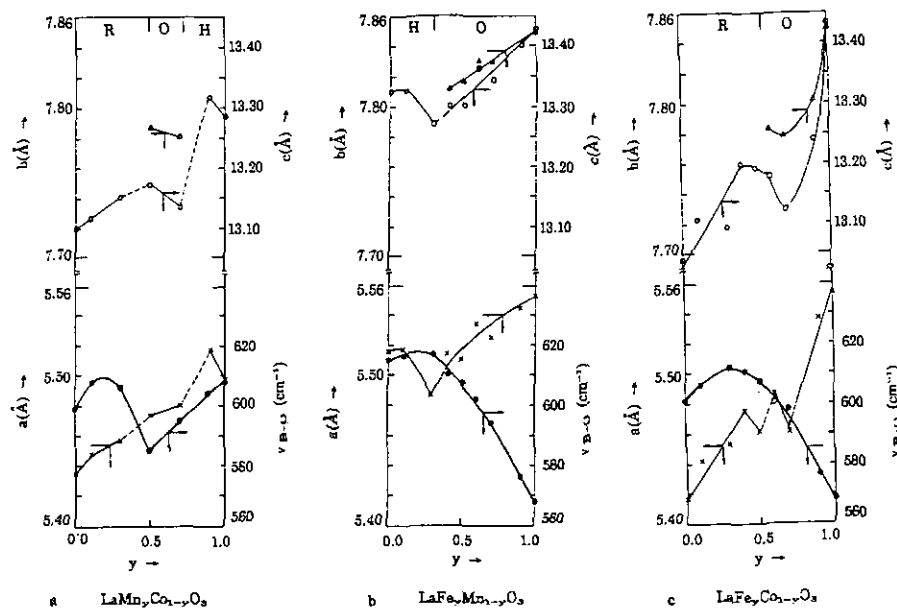


FIG. 1. The relationship between the lattice parameters, the stretching vibration frequency of infrared absorption, and the composition of different series.

### Infrared Spectra Investigation

IR spectroscopic investigation of these series produced an interesting pattern which seems to be related to the crystal phases.

The regular cubic perovskite structure belongs to the

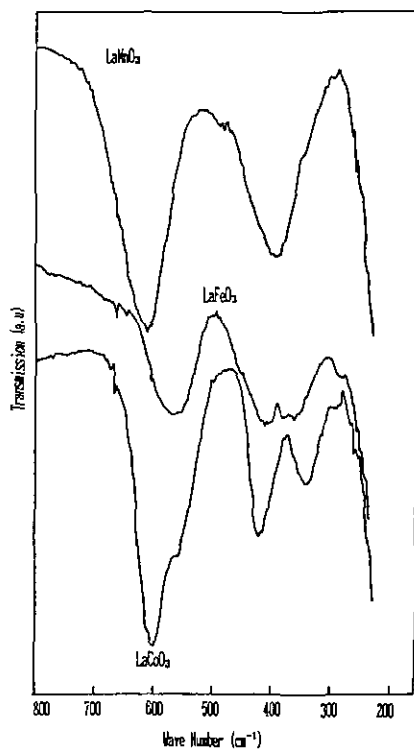


FIG. 2. Infrared absorption spectra of  $\text{LaMO}_3$  ( $M = \text{Mn, Fe, Co}$ ).

$O_h^1$  space group. From group theory, the optical active lattice vibrations are given by  $3F_{1u} + F_{2u}$  (10), of which the  $F_{2u}$  mode is inactive in the infrared region. Therefore the infrared spectra of the perovskite structure should show three absorption bands. These can be attributed to the B–O bond stretching vibration of the  $\text{BO}_6$  octahedra ( $\nu_1: F_{1u}$ ), to the bending vibration of the B–O bond ( $\nu_2: F_{1u}$ ), and to lattice vibrations ( $\nu_3: F_{1u}$ ), respectively. The expected band order is usually  $\nu_1 > \nu_2 > \nu_3$ . Any deviation from cubic symmetry causes splitting of these three bands.

Figure 2 depicts the observed spectra of the three mixed oxides. They are all spectra typical of the symmetry of the crystal phases. The hexagonal phase ( $\text{LaMnO}_3$ ) has two bands  $\nu_1$  and  $\nu_2$  (higher symmetry); splitting of the orthorhombic phase ( $\text{LaFeO}_3$ , lower symmetry) occurs at band  $\nu_2$  and in the rhombohedral phase ( $\text{LaCoO}_3$ ) there is not only splitting of band  $\nu_2$  but also a strong shoulder at the lower frequency side of  $\nu_1$  (lower symmetry). These results are similar to those reported by Subba *et al.* (9). The doping of foreign ions in each host mixed oxide obviously causes the shift and even splitting of the absorption bands, as shown in Figs. 3 to 5, and summarized in Fig. 1.

For the hexagonal phase ( $\text{LaMnO}_3$  and Mn-rich samples), there appears in the spectrum of  $\text{LaMnO}_3$  a shoulder ( $630 \text{ cm}^{-1}$ ) on the high-frequency side of the  $\nu_1$  band, due to its lower symmetry. The weak absorption between  $\nu_1$  and  $\nu_2$  bands changes into a shoulder at the  $\nu_2$  band upon doping with Co or Fe. The decrease of the frequency of the Mn–O stretching vibration ( $610\text{--}604 \text{ cm}^{-1}$ ) after doping with a small amount of Co ( $y = 0.9$ ) suggests that the covalency of the Mn–O bond is decreased and that the

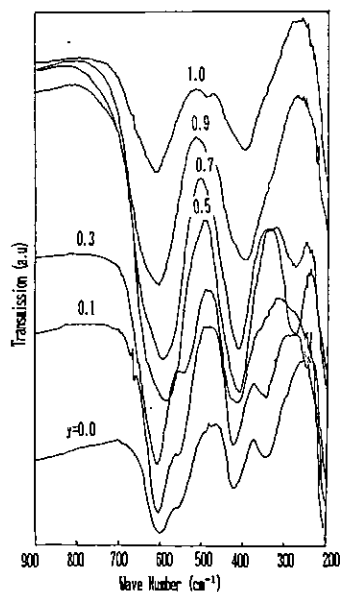


FIG. 3. Infrared absorption spectra of  $\text{LaMn}_y\text{Co}_{1-y}\text{O}_3$ .

ionicity is increased. In the case of Fe doping, the spectrum remains almost unchanged, showing that the influence of Fe on the Mn–O stretching vibration is not marked and that the lattice parameters also have not markedly changed. Nevertheless, the influence of Fe on the Mn–O bending vibration is notable.

For the rhombohedral phase ( $\text{LaCoO}_3$  and Co-rich samples), the frequency of the stretching vibration of the

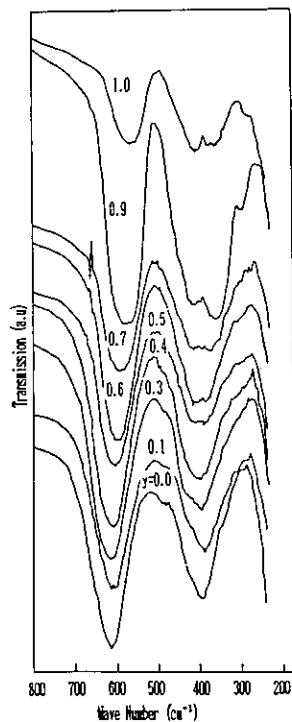


FIG. 4. Infrared absorption spectra of  $\text{LaFe}_y\text{Mn}_{1-y}\text{O}_3$ .

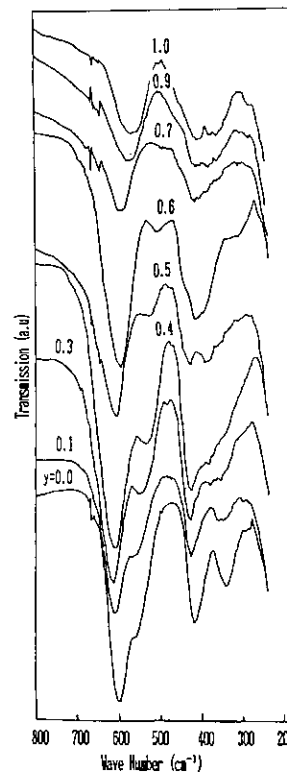


FIG. 5. Infrared absorption spectra of  $\text{LaFe}_y\text{Co}_{1-y}\text{O}_3$ .

Co–O bond increases with increasing amounts of Mn ( $599\text{--}608\text{ cm}^{-1}$ ) or Fe ( $601\text{--}615\text{ cm}^{-1}$ ). This means that the covalency of the Co–O bond becomes stronger with increasing concentrations of Mn or Fe in  $\text{LaCoO}_3$ . Correspondingly, the shoulder absorption at the  $\nu_1$  band shifts to lower frequencies with Mn doping and becomes more visible than that of  $\text{LaCoO}_3$  itself ( $558\text{--}550\text{ cm}^{-1}$ ). After doping Fe into  $\text{LaCoO}_3$ , the intensity of the peak at the lower frequency side of  $\nu_2$  band ( $346\text{--}358\text{ cm}^{-1}$ ) becomes weaker.

As for orthorhombic oxides, three bands are encountered in  $\text{LaMn}_{0.5}\text{Co}_{0.5}\text{O}_3$  and  $\text{LaMn}_{0.7}\text{Co}_{0.3}\text{O}_3$  samples. The stretching vibration frequency of the B–O bond is much lower than that of  $\text{LaMnO}_3$  and  $\text{LaCoO}_3$  (for  $y = 0.5$ ,  $585\text{ cm}^{-1}$ ;  $y = 0.7$ ,  $593\text{ cm}^{-1}$ ). This may be related to the strong interaction between Mn and Co ions (see below). The second ( $\nu = 410\text{ cm}^{-1}$ ) and the third absorption peaks ( $\nu = 275\text{ cm}^{-1}$ ) remain almost unchanged with the variation of composition. Because of the large distance between the two peaks ( $135\text{ cm}^{-1}$ ) these could not have been derived from a splitting of the  $\nu_2$  band. We believe that the second peak is due to the bending vibration of the B–O bond and the third peak to the lattice vibration ( $\nu_3$ ) related to the nature of the La–O bond.

The spectra of  $\text{LaFeO}_3$  and Fe-rich samples differ from those for the above two samples, even though both have the same crystal phase. A splitting of the  $\nu_2$  band is ob-

served; this may be due to the  $\nu_3$  band being upshifted. The stretching vibration frequency is close to  $568\text{ cm}^{-1}$ , which is  $20\text{--}30\text{ cm}^{-1}$  lower than that for  $\text{LaMnO}_3$  and  $\text{LaCoO}_3$ . This means that the covalency of the Fe–O bond is much lower than that of the Mn–O or Co–O bond. With an increase of Mn content in  $\text{LaFeO}_3$ , the frequency of  $\nu_1$  increases. This reflects the fact that the  $\nu_1$  mode results from the joint action of the Mn–O and Fe–O stretching motions: since the Mn–O bonds vibrate at a higher frequency the resulting mode is upshifted in proportion to the presence of Mn–O bonding. This also corresponds to a decrease of the lattice parameters when doping with Mn in  $\text{LaFeO}_3$  (Fig. 1). The frequency close to  $426\text{ cm}^{-1}$  does not change much with an increase in Mn content. Since the change of the B-ion state does not strongly influence the A ion, this absorption peak may be related to the characteristics of the La–O bond. The frequency near  $370\text{ cm}^{-1}$  increases with Mn content; this change may be interpreted in the same manner as that for the  $\nu_1$  band.

The case of  $\text{LaFe}_y\text{Co}_{1-y}\text{O}_3$  is very similar to that of  $\text{LaFe}_y\text{Mn}_{1-y}\text{O}_3$ . Doping with Co also leads to an increase of the frequencies of the stretching vibration ( $568\text{--}600\text{ cm}^{-1}$ ) and of the bending vibration ( $411\text{--}418\text{ cm}^{-1}$ ) of the Fe–O bond as well as to a decrease of lattice parameters. The only difference between them is that close to about  $650\text{ cm}^{-1}$  there is a sharp absorption peak. Its frequency does not change with variations of occupancy of the B site.

At present, we cannot decide which parameter is mainly responsible for the observed frequency shift. In such an isomorphic substitution system the following four parameters can all modify the vibrational frequencies: (1) the mass of the cation B, (2) its ionic radius and, thus, the B–O distance, (3) the electronic structure of the cation, and (4) the cation–oxygen bonding force. Nevertheless, we can classify these four parameters in two categories, geometrical (1 and 2) and electronic (3 and 4), which, in

turn, might be related to the observed frequency shift, as follows:

*Geometrical:* (a) Lattice parameter decreases, B–O bond becomes shorter, B–O frequency becomes larger; (b) lattice parameter increases with the opposite effects.

*Electronic.* (a) Ion B as electron donor: covalency of B–O decreases, ionicity of B–O increases, frequency decreases; (b) Ion B as electron acceptors with the opposite effects.

Considering the results in Fig. 1, we conclude that the principal factor responsible for the shift seems to be different in each case. That is, for the Mn–Co system, the electronic factors may be dominant, but for the Fe-containing system, the geometrical factors predominate.

#### ACKNOWLEDGMENT

This work was supported by the National Natural Science Foundation of China.

#### REFERENCES

1. L. G. Tejuca, J. L. G. Fierro, and J. M. D. Tascon, in "Advances in Catalysis, Vol. 36" (D. D. Eley, H. Pines, and P. B. Weisz, Eds.), p. 237.
2. Y. Wu *et al.*, *J. Catal.* **120**, 88 (1989).
3. J. T. Last, *Phys. Rev.* **105**, 1740 (1957).
4. A. I. Stekhanov and A. A. Karamyan, *Sov. Phys. Solid State* **8**, 355 (1966).
5. C. P. Perry, B. N. Khanna, and G. Rupprecht, *Phys. Rev. A* **135**, 408 (1964).
6. C. H. Perry, D. J. McCarthy, and G. Rupprecht, *Phys. Rev. A* **138**, 1537 (1965).
7. D. Krol and G. Blasse, *J. Inorg. Nucl. Chem* **37**, 1328 (1975).
8. Von I. L. Botto and E. J. Baran, *Z. Anorg. Allg. Chem.* **473**, 189 (1981).
9. G. V. Subba, C. N. R. Rao, and J. R. Ferraro, *Appl. Spectrosc.* **24**(4), 436 (1970).
10. A. P. Lane, D. W. A. Sharp, J. M. Barraclough, D. H. Brown, and D. A. Paterson, *J. Chem. Soc. A*, 94 (1971).